THEORETICA CHIMICA ACTA
Theoret. Chim. Acta (Berl.) 63, 323–338 (1983)

Chemical Applications of Topology and Group Theory

14. Topological Aspects of Chaotic Chemical Reactions*

R. B. King

Department of Chemistry, University of Georgia, Athens, GA 30602, USA

Earlier approaches to the analysis of chemical dynamic systems using kinetic logic are refined to deal more effectively with systems having the two or more feedback circuits required for chaos. The essential kinetic features of such a system can be represented by a directed graph (called an *influence diagram*) in which the vertices represent the internal species and the directed edges represent kinetic relationships between the internal species. Influence diagrams characteristic of chaotic chemical systems have the following additional features: (1) They are connected; (2) Each vertex has at least one edge directed towards it and one edge directed away from it; (3) There is at least one vertex, called a turbulent vertex, with at least two edges directed towards it. From such an influence diagram a state transition diagram representing the qualitative dynamics of the system can be obtained using the following 4-step procedure: (1) A logical relationship is assigned at each turbulent vertex; (2) A local truth table is generated for each circuit in the influence diagram; (3) The local truth tables are combined to give a global truth table using the logical relationships at the turbulent vertices; (4) The global truth table is used to determine the corresponding state transition diagram using previously described methods. This refined procedure leads to a more restricted set of influence diagrams having the interlocking cycle flow topology required for chaos than the procedure described earlier. Systems with 3 internal species are examined in detail using the refined procedure. All systems with 3 dynamic variables shown in the simulation studies of Rössler to give chaotic dynamics correspond to influence diagrams which give interlocking cycle (chaotic) flow topologies by the refined procedure. In addition, two models for the Belousov–Zhabotinskii reaction are examined using the

* For part 13 of this series see R. B. King, Theoret. Chim. Acta (Berl.) 63, 103–132 (1983)

refined procedure. The results are potentially informative concerning possible mechanisms for the limitation of the accumulation of autocatalytically produced $HBrO_2$ (one of the internal species) during the course of this reaction.

Key words: Dynamic systems – Chaotic chemical reactions – Kinetic logic – Turbulence – Belousov–Zhabotinskii reaction.

1. Introduction

During the past decade, chemical reactions exhibiting periodic oscillatory behavior have attracted increasing attention [1, 2, 3]. More recently, the possibility that the oscillations in such reactions may become aperiodic (chaotic) has been raised. Hudson and coworkers [4–6] report conditions where the oscillations of the Belousov–Zhabotinskii reaction in a continuous-flow stirred reactor appear to become chaotic. Using an early work of Lorenz [7] as an initial guide, Rössler [8–12] has found several different sets of three simultaneous differential equations which exhibit chaotic behavior in simulation studies.

These experimental observations on oscillating and chaotic chemical reaction networks have stimulated continuing interest in the mathematics of such systems. In this connection the following two general approaches appear to be emerging for the analysis of complicated sets of potentially oscillating and/or chaotic differential equations: (1) Clarke [13, 14] has developed a graph theoretical approach for the determination of the stability of steady states; (2) Switching circuit theory [15, 16] has been used to analyze [17–22] the flow topology [23] around unstable steady states; this approach has been called *kinetic logic* [24]. This paper presents a refinement of earlier approaches [23, 25] to the kinetic logic of multiple feedback circuit kinetic systems of types which are potential candidates for chaotic behavior.

2. General Background

The most convenient terms for classifying species found in chemical reaction networks are internal and external species [14]. The concentrations of *internal species* (also called *reference reactants*) vary on the time scale of interest and therefore are dynamical variables. The concentrations of *external species* (also called *major reactants*) remain sufficiently close to a constant on the time scale of interest to be omitted as dynamical variables.

The concentrations of the internal species in a chemical system can be represented by the variables $x_1, x_2, \ldots, x_n$. The position of the system can always be defined by a point in the positive orthant of n-dimensional concentration space R^n. A *steady state* of this system is defined by

$$\dot{x}_1 = \dot{x}_2 = \cdots = \dot{x}_n = 0 \tag{1}$$

where the dots refer to the time derivatives $dx_1/dt, dx_2/dt, \ldots, dx_n/dt$. Such a steady state is *stable* if all nearby solutions stay nearby for all future time [26].

Stable steady states are clearly significant by indicating where a dynamic system will come to rest. The significance of unstable steady states in determining dynamic behavior depends upon their neighborhoods, i.e., their *flow topologies.* In a two-variable system (i.e. $n = 2$) in which a third dimension represents energy, a stable steady state represents a pit and an unstable steady state represents a peak or saddle point.

In the treatment in this paper as in previous work [23, 25] the relationship between the internal species is represented by a directed graph [27] called an *influence diagram.* An influence diagram has one vertex for each internal species. An edge is directed from a vertex representing a given internal species to a vertex representing an internal species whose rate of concentration change is affected by the first internal species. Such a directed edge is given a positive or negative weight if the relationship is activation or inhibition, respectively. If a given internal species has no effect on another given internal species, then the corresponding directed edge vanishes. A *class* of influence diagrams consists of all such diagrams which become equivalent when vertex labels are dropped. All members of the same class of influence diagrams have flow topologies of the same type. A *family* of influence diagrams consists of all classes of influence diagrams which become identical when edge labels are dropped. All members of the same family of influence diagrams do *not* necessarily have flow topologies of the same type.

The circuits in influence diagrams are important in the treatment of this paper. A *circuit* in an influence diagram consists of a path which starts with a given vertex and follows various edges in the directions of the arrows until the original vertex is reached again. The *length* of a circuit is the number of edges in the circuit that must be traversed from a given vertex until that same vertex is reached again. A circuit is *negative* if it has an odd number of negative edges and *positive* if it has an even number of negative edges or no negative edges. Following previous practice [23, 25], positive and negative circuits of length n are called B_n and C_n circuits, respectively.

In a search for influence diagrams which can represent chaotic chemical systems, only influence diagrams of a special type called turbulent influence diagrams need to be considered. A *turbulent influence diagram* has the following three properties:

(1) There is a path between every pair of vertices, i.e. the diagram is connected.

(2) Each vertex has at least one edge directed towards it and one edge directed away from it.

(3) There is at least one vertex, called a *turbulent vertex*, with at least two edges directed towards it.

Influence diagrams having only the first two properties listed above have been called oscillatable [23] or strong [25] influence diagrams. They have been considered in my earlier papers on the flow topology of oscillating reactions [23, 25].

This paper discusses chemical dynamic systems having 3 internal species. The following 4 families of turbulent influence diagrams are possible for systems having 3 internal species:

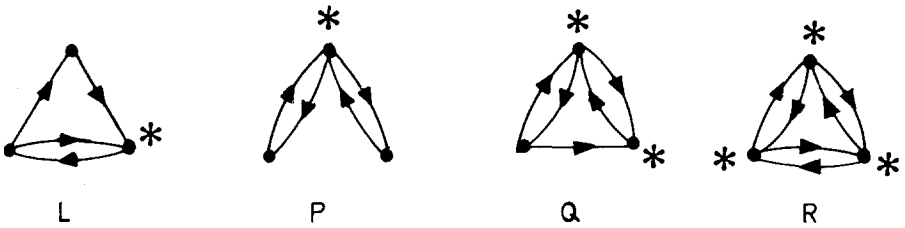

The letters labelling the families are taken from an earlier paper [23] and the turbulent vertices are starred. The families L, P, and Q are all treated explicitly in this paper. Similar methods are also applicable to family R, which is significantly more complicated since it has all possible circuits and all 3 vertices are turbulent.

3. The Flow Topology of Chemical Systems Represented by Turbulent Influence Diagrams

Consider the chemical system represented by an influence diagram as a synchronous switching network in which time is quantized so that the signs of the first time derivatives of the concentrations of the internal species at time $t+1$ are determined by their signs at time t [18, 19]. The switching state at any time of such a chemical system containing n internal species can be represented by an n-vector of 1's and 0's corresponding to positive and negative time derivatives, respectively, of the concentrations of each of the n internal species. Such an n-vector is called a *state vector.* The number of different possible state vectors in an n-dimensional system is 2^n and these state vectors can be represented by the 2^n vertices of an n-dimensional cube. The possible transitions from states at synchronous time t to those at time $t+1$ may then be represented by arrows directed along the edges of the n-cube. In such transitions the value of exactly one component of the state vector changes. Furthermore in this treatment the discrete time scale t is chosen so that it advances one unit each time a single component of the state vector changes. The resulting n-cube with directed edges is called a *state transition diagram.* The center of the n-cube representing a state transition diagram corresponds to a steady state at which all of the first time derivatives of the concentrations of the internal species are zero (Eq. 1) and therefore do not correspond to either Boolean variable 0 or 1. If this steady state is unstable, the transitions represented by the directed edges of the state transition diagram define the fundamental topology of the flow in the neighborhood of the unstable steady state.

The calculations of state transition diagrams corresponding to a given turbulent influence diagram can be performed by the following four-step procedure:

(1) A logical relationship (AND or OR) is assigned between the set of edges directed towards a given turbulent vertex. Since each of these two logical

relationships (AND, OR) at a turbulent vertex leads to a separate state transition diagram, the total number of state transition diagrams for a given turbulent influence diagram with v turbulent vertices is 2^v. This number can become still larger if more than two edges are directed towards some of the turbulent vertices and more complicated logical relationships are allowed between three or more edges directed towards a given turbulent vertex.

(2) A *local truth table* is generated for each circuit in the influence diagram to indicate possible transitions between state vectors. In order to see how such a local truth table is generated, consider possible effects of one internal species X on a second internal species Y. If X activates Y as indicated by a positive arrow from X to Y in the circuit under consideration, then in the local truth table the values for Y in each possible state vector at time $t+1$ will correspond to values for X at time t. Thus when X activates Y an increase in the concentration of X (represented by 1 in the state vector coordinate) leads eventually to an increase in the concentration of Y (also represented by 1 in the state vector coordinate) and vice versa. However, if X inhibits Y as indicated by a negative arrow from X to Y in the circuit under consideration, then in the local truth table the values for Y at time $t+1$ will be the opposite of the values for X at time t (i.e. a 0 for x at time t leads to a 1 for Y at time $t+1$ and vice versa). Thus in the absence of other effects when X inhibits Y, an increase in the concentration of X (represented by 1 in the corresponding state vector coordinate) eventually leads to a decrease in the concentration of Y (represented by 0 in the corresponding state vector coordinate) and vice versa.

(3) The local truth tables for each of the circuits in the turbulent influence diagram are combined to give a *global truth table* using the local relationships at the turbulent vertices as follows:
(a) If any of the local truth tables show a value of 0 for a variable represented by an AND turbulent vertex, then the global truth table for that variable also shows a value of 0.
(b) If any of the local truth tables show a value of 1 for a variable represented by an OR turbulent vertex, then the global truth table for that variable also shows a value of 1.

(4) The global truth table is used to determine the corresponding state transition diagram using the following algorithm:
(a) Select two state vectors corresponding to an edge of the n-cube representing the state transition diagram and the state of the system at time t. Such a pair of state vectors will be identical except for one component called the *switching component.*
(b) Advance the discrete time scale by one unit and compare the switching components in the corresponding state vectors at discrete time $t+1$ as indicated by an appropriate row in the global truth table. If both switching components are 0 at time $t+1$, then the arrow on the corresponding edge of the state transition diagram will be directed towards the vertex corresponding to the state vector at time t where the switching component is 0. If both switching components

are 1 at time $t+1$, then the arrow on the corresponding edge of the state transition diagram will be directed towards the vertex corresponding to the state vector at time t where the switching component is 1. The third and remaining possibility where the switching component at time $t+1$ is 0 for one state vector and 1 for the other state vector implies the assignment of both edge directions on the corresponding edge of the transition diagram. This third possibility only arises when considering a feedback circuit not containing the switching component.
(c) Repeat this procedure for the other pairs of state vectors corresponding to the remaining edges of the n-cube until all edges have been considered.

Steps 2 and 4 of the above procedure are based on work by Glass [17–22] and have been used by the author in his previous papers [23, 25]. Steps 1 and 3 of the above procedure are suggested by the work of Thomas [24] and involve only the turbulent vertices. They vanish when strong influence diagrams containing only one circuit (i.e. fundamental polygons [25]) are considered, since such influence diagrams have no turbulent vertices. Also the author has considered the properties of state transition diagrams derived from turbulent influence diagram when no logical structure is imposed at any of the turbulent vertices so that *all* edge directions on the state transition diagram implied by individual circuits are regarded as possible in the global sense [23, 25]. Such state transition diagrams (called *free* state transition diagrams [25]) lead to many more systems having the interlocking cycles required for chaotic behavior than the state transition diagrams with logical constraints at the turbulent vertices considered in this paper. Since the analysis of flow topology gives necessary rather than sufficient conditions for interesting dynamic behavior such as oscillations and chaos, a theory which predicts a smaller number of cases for a given type of interesting dynamic behavior is more useful provided, of course, the theory is correct.

The remainder of this paper demonstrates the following features of the flow topologies obtained from turbulent influence diagrams when logical relationships are imposed on turbulent vertices as outlined above:

(1) In most of the important cases the qualitative features of the flow topology indicated by the state transition diagram remain unchanged when an AND relationship at a turbulent vertex is changed to an OR relationship. This change in logical relationship may change only the *location* in the state transition diagram of dynamically significant features such as vertices representing attracting regions or interlocking cycles representing chaos. Thus the predictions of this theory are relatively insensitive to the correctness of the logical relationships assigned to the turbulent vertices so that a fairly arbitrary assignment of logical relationships appears satisfactory for most purposes.

(2) The number of turbulent influence diagrams leading to state transition diagrams having interlocking cycles becomes much smaller when logical structure is imposed on the turbulent vertices (as compared with free state transition

diagrams as defined above). However, *all* dynamic systems observed to exhibit chaos in computer modelling studies correspond to one of the much smaller number of turbulent influence diagrams exhibiting the interlocking cycle chaotic flow topology using the more restrictive algorithm outlined in this paper as compared with the earlier work [23, 25] using free state transition diagrams. The theory outlined in this paper thus represents a useful refinement of the earlier theories [23, 25].

The four-step procedure outlined above for obtaining a state transition diagram from a turbulent influence diagram is illustrated in Table 1 for a C_2+C_2 system,

Table 1. Calculations of state transition diagrams for a C_2+C_2 turbulent influence diagram

(*A*) *Influence diagram*
Turbulent vertex at Y

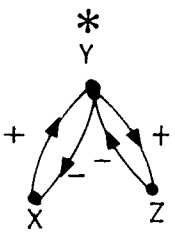

(*B*) *Truth tables*

	Local truth table		Global truth table	
	Left circuit	Right circuit	AND at Y	OR at Y
Time t	Time $t+1$	Time $t+1$	Time $t+1$	Time $t+1$
$x\ y\ z$	$x\ y\ z$	$x\ y\ z$	$x\ y\ z$	$x\ y\ z$
0 0 0	1 0 −	− 0 1	1 0 1	1 0 1
1 0 0	1 1 −	− 0 1	1 0 1	1 1 1
0 1 0	0 0 −	− 0 0	0 0 0	0 0 0
0 0 1	1 0 −	− 1 1	1 0 1	1 1 1
1 1 0	0 1 −	− 0 0	0 0 0	0 1 0
1 0 1	1 1 −	− 1 1	1 1 1	1 1 1
0 1 1	0 0 −	− 1 0	0 0 0	0 1 0
1 1 1	0 1 −	− 1 0	0 1 0	0 1 0

(*C*) *State transition diagrams*

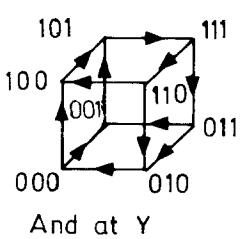

And at Y

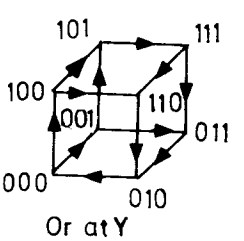

Or at Y

the simplest system exhibiting a state transition diagram having the interlocking cycles required for chaotic behavior. The four steps listed above are performed as follows in this case:

(1) The C_2+C_2 system depicted in Table 1 has one turbulent vertex, namely Y. Therefore 2 state transition diagrams can be obtained from this system depending upon whether the logical relationship at Y is AND or OR. These 2 state transition diagrams are depicted at the bottom of Table 1.

(2) Separate local truth tables are calculated for the left circuit consisting of X and Y and for the right circuit consisting of Y and Z. Thus the local truth table for the left circuit contains no entry for Z and the local truth table for the right circuit contains no entry for X since these vertices are absent from the circuit under consideration.

(3) The global truth table differs only in the entries in the columns for Y since this is the only turbulent vertex. Thus in the four cases where one of the local truth tables has a 0 entry for Y and the other local truth table has a 1 entry for Y, the global truth table for an AND relationship at Y has a 0 entry and the global truth table for an OR relationship at Y has a 1 entry.

(4) Both of the state transition diagrams have interlocking cycles of lengths 4 and 6. In the state transition diagram for an AND relationship at Y the cycles of length 4 are located on the top and rear faces of the cube and a cycle of length 6 follows the path 000–100–101–111–011–010–000. Similarly in the state transition diagram for an OR relationship at Y, the cycles of length 4 are located on the front and bottom faces of the cube and a cycle of length 6 follows the same path (000–100–101–111–011–010–000) as the corresponding cycle on the state transition diagram for an AND relationship at Y. Thus changing the logical relationship at Y from AND to OR in the C_2+C_2 influence diagram does not affect the position of the cycle of length 6 on the corresponding state transition diagram but only the positions of the cycles of length 4.

Table 2 summarizes the results of such calculations of state transition diagrams having one or two turbulent vertices. Table 2 also illustrates the effects of logical structure at the turbulent vertices on the resulting flow topologies.

The flow topologies of the 3-variable state transition diagrams arising from calculations with or without logical structure at the turbulent vertices are all of one of the following four types:

(1) *Two Attracting Regions.* Two diagonally opposite vertices of the cube each have all three edges directed towards the vertex in question thereby representing the signs of the time derivatives in the attracting regions.

(2) *One Attracting Region.* A single vertex of the cube has all three edges directed towards itself thereby representing the signs of the time derivatives in an attracting region. This flow topology only arises when logical structure is imposed at turbulent vertices since it is symmetry forbidden [25] in free state transition diagrams.

Table 2. The effect of logical structure at turbulent vertices on the flow topologies of 3-variable state transition diagrams

Influence diagram Circuit structure	Flow topology of state transition diagram	
	Free	Logical structure
B_2+B_2	2 attracting regions	2 attracting regions
B_2+C_2	interlocking cycles	1 attracting region
C_2+C_2	interlocking cycles	interlocking cycles
B_2+B_3	2 attracting regions	2 attracting regions
B_2+C_3	cyclic attractor	1 attracting region
C_2+B_3	interlocking cycles	1 attracting region
C_2+C_3	interlocking cycles	interlocking cycles
$B_2+B_2+B_3$	2 attracting regions	2 attracting regions
$B_2+B_2+C_3$	cyclic attractor	1 attracting region
$B_2+C_2+B_3$	interlocking cycles	1 attracting region
$B_2+C_2+C_3$	interlocking cycles	1 attracting region or interlocking cycles (see text)
$C_2+C_2+B_3$	interlocking cycles	1 attracting region or interlocking cycles (see text)
$C_2+C_2+C_3$	interlocking cycles	interlocking cycles

(3) *Cyclic Attractor.* A single cycle of length 6 is formed. The two vertices not in this cycle each have all three edges directed away from them towards the vertices forming the cycle. This flow topology represents periodic oscillations and does not arise from turbulent influence diagrams when logical structure is imposed at the turbulent vertices.

(4) *Interlocking Cycles.* Cycles of lengths 4 and 6 are found which have edges in common. There are no vertices which have all three edges directed towards the vertex in question, i.e., attracting regions are absent. This flow topology represents chaos since the interlocking cycles can prevent the oscillations from having a definite period.

The following conclusions can be derived from the information in Table 2:

(1) For influence diagrams having exactly one turbulent vertex (i.e. those in Table 2 with 2 circuits) the flow topology type is independent of the logical structure (AND, OR) at the turbulent vertex.

(2) For influence diagrams having 2 turbulent vertices (i.e. those in Table 2 having 3 circuits) the flow topology type may depend only upon whether the 2 turbulent vertices have the same or different logical structures. Furthermore, this factor is only critical for the $B_2+C_2+C_3$ and $C_2+C_2+B_3$ systems where in Table 2 the first flow topology type listed (1 attracting region) arises when the two turbulent vertices have the same logical structure (AND + AND or OR + OR) and the second flow topology listed (interlocking cycles) arises when the two turbulent vertices have different logical structures (AND + OR).

(3) *Free* state transition diagrams derived from an influence diagram with n vertices have interlocking cycles any time a C_{n-1} circuit is present [25]. Thus all influence diagrams in Table 2 having C_2 circuits exhibit the interlocking cycle flow topology for their *free* state transition diagrams. In particular the flow topology of such systems is insensitive to added B_2 and B_3 circuits if a C_2 circuit is present. Such is no longer true when logical structure is imposed on the turbulent vertices where a C_2+C_2 or C_2+C_3 circuit pair is required to produce interlocking cycle flow topology. Thus turbulent influence diagrams having 3 vertices and only *one* C_2 circuit which exhibit interlocking cycle flow topology when their *free* state transition diagrams are considered instead exhibit flow topology with one attracting region when logical structure is imposed on the turbulent vertices.

A major conclusion from the analysis in this paper is that imposition of logical structure on the turbulent vertices of influence diagrams reduces significantly the range of systems exhibiting the interlocking circuit flow topology necessary for a chaotic system. This added feature therefore sharpens the predictive value of flow topology for identifying dynamic systems with the potential for chaotic behavior. The next section of this paper compares the predictions of this theory with actual dynamic systems for which chaotic behavior has been demonstrated.

4. Comparison with Simulation Studies

Rössler has found a variety of systems of 3 differential equations which exhibit chaos in simulation studies. These systems are listed in Table 3 along with a summary of their influence diagram types and non-linearities.

Comparison of Table 3 with Table 2 reveals that all of the 3-variable systems shown to exhibit chaos in simulation studies correspond to turbulent influence diagrams giving state transition diagrams having the interlocking cycles required for chaos even when logical structure is imposed on the turbulent vertices. Most of the systems in Table 3 correspond to C_2+C_2 influence diagrams but there are also examples of systems having $B_2+C_2+C_3$, $C_2+C_2+C_3$, and C_2+C_3 influence diagrams with feasible parameter values in some feasible region of concentration space. Thus all of the 3-variable turbulent influence diagrams with logical structure shown to have interlocking cycle (chaotic) flow topologies in Table 2 are represented in Table 3 except for the $C_2+C_2+B_3$ system. Furthermore, none of the examples of actual chaotic dynamic systems in Table 3 correspond to influence diagrams which give state transition diagrams having flow topologies other than the interlocking cycle flow topology when logical structure is imposed at the turbulent vertices. Thus the B_2+C_2, C_2+B_3, and $B_2+C_2+B_3$ influence diagrams do not appear in Table 3; these are the 3-variable influence diagrams which give *free* state transition diagrams having interlocking cycles but state transition diagrams having 1 attracting region when logical structure is imposed. This suggests that the imposition of logical structure at the turbulent vertices improves the value of this theory for predicting dynamic systems leading to chaos.

Table 3. Three-variable dynamic systems shown to exhibit chaos in simulation studies

System	Influence diagram type	Nonlinear equations[a]	Reference
$\dot{x} = 10(y-x)$ $\dot{y} = x(28-z)-y$ $\dot{z} = xy - \frac{8}{3}z$	$B_2+C_2+C_3$ or $C_2+C_2+C_3$	2Q	Lorenz[b]
$\dot{x} = -(y+z)$ $\dot{y} = x+0.2y$ $\dot{z} = 0.2+z(x-5.7)$	C_2+C_2	1Q	Rössler[c]
$\dot{x} = a+bx-(cy+dz)x/(x+K)$ $\dot{y} = ex-fb$ $\dot{z} = yx+hz-jz^2-mz/(z+K')$	C_2+C_2	1Q+1C	Rössler[d]
$\dot{x} = x-xy-z$ $\dot{y} = x^2-ay$ $\dot{z} = bx-cz+d$	C_2+C_2	2Q	Rössler[e]
$\dot{x} = -y-z$ $\dot{y} = x+ay$ $\dot{z} = b+xz-cz$	C_2+C_2	1Q	Rössler[e]
$\dot{x} = -y+ax-bz$ $\dot{y} = x+1.1$ $\dot{z} = c(1-z^2)(x+z)-z$	C_2+C_2 or B_2+C_2	1C	Rössler[f]
$\dot{x} = -y-z$ $\dot{y} = x+ay$ $\dot{z} = bx-cz+xz$	C_2+C_2	1Q	Rössler[f]
$\dot{x} = x-xy-z$ $\dot{y} = x^2-ay$ $\dot{z} = b(cx-z)$	C_2+C_2	2Q	Rössler[f]
$\dot{x} = -xy-ax-z$ $\dot{y} = -x+by+cz$ $\dot{z} = d+exz+fx$	$B_2+C_2+C_3$	2Q	Rössler[f]
$\dot{x} = -y-z$ $\dot{y} = x$ $\dot{z} = a(y-y^2)-bz$	C_2+C_3 or C_2+B_3	1Q	Rössler[f]

[a] This refers to the number of the three equations that have quadratic (Q) or cubic (C) terms as the highest degree terms rather than linear terms

[b] Lorenz, E. N.: J. Atmos. Sci. **20**, 130 (1963)

[c] Rössler, O. E.: Phys. Letters **57A**, 397 (1976)

[d] Rössler, O. E.: Z. Naturforsch. **31a**, 259 (1976)

[e] Rössler, O. E.: Z. Naturforsch. **31a**, 1664 (1976)

[f] Rössler, O. E.: Ann. N. Y. Acad. Sci. **316**, 376 (1979)

The following features of Table 3 are also of interest:

(1) Some of the dynamic systems in Table 3 correspond to different influence diagrams in different regions of concentration space, i.e., they are composite rather than simple chemical systems [23]. Thus the first system in Table 3 is a

$B_2+C_2+C_3$ system when $z<28$ and a $C_2+C_2+C_3$ system when $z>28$. Similarly the sixth system is a C_2+C_2 system when $z<1$ and a B_2+C_2 system when $z>1$.

(2) All of the systems in Table 3 have at least one non-linear differential equation. In most cases this non-linear equation is quadratic (including xy, yz, or xz terms which become quadratic when solving for x, y, and z values at the steady states $\dot{x}=\dot{y}=\dot{z}=0$). This non-linearity is needed to provide at least 2 steady states so that there will be at least one *unstable* steady state in the positive octant of concentration space. The analysis of flow topology in this and previous [23, 25] papers is meaningful only when there is an unstable steady state in the positive octant of concentration space around which the predicted flows can occur. The simplest type of dynamic system which can exhibit chaos is the simple C_2+C_2 3-variable system having one quadratic and 2 linear equations as exemplified by the second, fifth, seventh, and eighth systems in Table 3.

5. Treatment of Models for the Oscillating Belousov–Zhabotinskii Reaction

The most thoroughly studied oscillating reaction is the Belousov–Zhabotinskii reaction which has the principal overall stoichiometry [28]:

$$2BrO_3^- + 3CH_2(CO_2H)_2 + 2H^+ \rightarrow 2BrCH(CO_2H)_2 + 3CO_2 + 4H_2O. \qquad (2)$$

The course of this reaction involves 3 major processes [29]:

(1) Reduction of BrO_3^- to Br_2 by oxygen atom transfers through $HBrO_2$ and HOBr followed by bromination of the malonic acid.

(2) Reduction of BrO_3^- to Br_2 by an autocatalytic process involving one electron transfers and free radical oxybromine intermediates using Ce^{+3} as an electron source. Again the resulting Br_2 brominates the malonic acid.

(3) Oxidation of bromomalonic acid and other organic bromine compounds with Ce^{+4} to regenerate Ce^{+3} and Br^-.

The internal species determining the phase of the system can be taken to be $HBrO_2$, Br^-, and Ce^{+4}; thus this system can be analyzed as a 3-variable system. Oscillations in this system are normally observed experimentally [30] by monitoring the concentrations of Br^- and/or Ce^{+4} as a function of time by using appropriate electrodes. The species BrO_3^-, malonic acid, total cerium, and organic oxidation products may be regarded as external species whose concentrations remain constant or nearly constant for a long time relative to the time of the oscillations.

In order to illustrate the application of the methods in this and previous [23, 25] papers to actual chemical dynamic systems, two models of the Belousov–Zhabotinskii reaction are examined. These models are summarized in Table 4. Both of these models contain 3 internal species $HBrO_2$, Br^-, and Ce^{+4}, which are designed as x, y, and z, respectively.

In order to obtain useful influence diagrams, only relationships between *different* internal species need to be considered. Self-activation and self-inhibition

Table 4. Two models for oscillations in the Belousov–Zhabotinskii reaction

Model[a]	Influence diagram[b]	Influence diagram type	Nonlinear equations[c]	Reference
$\dot{x} = ay - xy + x - x^2$ $\dot{y} = -ay - xy + bz$ $\dot{z} = x - z$	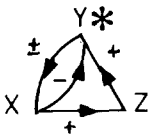	$C_2 + B_3(x < a)$ $B_2 + C_3(x > a)$	2Q	[d]
$\dot{x} = (1-a)x + y - xy - xz$ $\dot{y} = -(1-a)y + z - xy + b$ $\dot{z} = -(1+ac)ez + ex - exz$	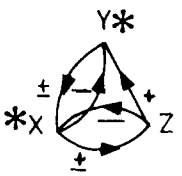	$C_2 + C_2 + B_3(x < 1, z < 1)$ $C_2 + B_2 + C_3(x < 1, z > 1)$ $B_2 + C_2 + C_3(x > 1, z < 1)$ $B_2 + B_2 + B_3(x > 1, z > 1)$	3Q	[e]

[a] In both models x, y, and z correspond to the concentrations of $HBrO_2$, Br^-, and Ce^{+4}, respectively. These are the internal species (reference reactants) in the Belousov–Zhabotinskii reaction. The malonic acid, bromate, and total cerium reactants and the various oxidation and bromination products of malonic acid are external variables which are incorporated in the above constants by procedures given in the cited references

[b] The turbulent vertices are starred

[c] Q refers to the number of quadratic equations in the dynamic system; the remaining equation in the first system (that for $\dot{z}$) is linear

[d] Tyson, J. J.: Ann. N. Y. Acad. Sci. **316**, 279 (1979)

[e] Tomita, K., Tsuda, I.: Phys. Letters **71A**, 489 (1979)

relationships are significant and important in the analysis of stability [13, 14] but not in the analysis of flow topology.

The influence diagrams for the models in Table 4 contain directed edges representing some of the following five chemical reactions in the overall mechanism for the Belousov–Zhabotinskii reaction:

(1) $y \xrightarrow{+} x$ (the y term in the $\dot{x}$ equation): the formation of $HBrO_2(x)$ by reaction of BrO_3^- (an external species) with $Br^-(y)$.

(2) $y \xrightarrow{-} x$ and $x \xrightarrow{-} y$ ($-xy$ terms in the $\dot{x}$ and $\dot{y}$ equations): the reaction of $HBrO_2(x)$ with $Br^-(y)$ to give HOBr.

(3) $z \xrightarrow{-} x$ and $x \xrightarrow{-} z$ ($-xz$ terms in the $\dot{x}$ and $\dot{z}$ equations): the accumulation of autocatalytically produced $HBrO_2(x)$ is limited by its oxidation with $Ce^{+4}(z)$. This feature only occurs in the Tomita and Tsuda model [31]. The $-x^2$ term in the $\dot{x}$ equation of the Tyson model [29] plays an analogous role and represents the limitation of the accumulation of autocatalytically produced $HBrO_2(x)$ through its bimolecular disproportionation into BrO_3^- and HOBr.

(4) $z \overset{+}{\rightarrow} y$ (z term in the $\dot{y}$ equation): the generation of $Br^-(y)$ by oxidation of organic bromine compounds (external variables) with $Ce^{+4}(z)$.

(5) $x \overset{+}{\rightarrow} z$ (x term in the $\dot{z}$ equation): the regeneration of $Ce^{+4}(z)$ from Ce^{+3} by oxidation with BrO_3^- (an external species) catalyzed by $HBrO_2(x)$.

Reactions 2 and 3 involve a bimolecular reaction between two internal species and therefore correspond to two negative edges in the influence diagram forming a B_2 circuit with the two internal species at the vertices. Also the simultaneous occurrence of reactions 1 and 2 leads to conflicting signs on the $y \rightarrow x$ directed edge and the simultaneous occurrence of reactions 3 and 5 leads to conflicting signs on the $x \rightarrow z$ directed edge. These systems may thus be regarded as composite chemical systems with different influence diagrams in different regions of concentration space.

The Tyson model [29] in Table 4 includes reactions 1, 2, 4, and 5 listed above and leads to an influence diagram having one turbulent vertex (Y) and 4 distinct directed edges, one of which can be either positive or negative. The Tomita and Tsuda model [31] in Table 4 includes all 5 reactions listed above and leads to a somewhat more complicated influence diagram having 2 turbulent vertices (X and Y) and 5 distinct directed edges, two of which can be either positive or negative. These 2 models differ essentially only in the way that the autocatalytic buildup of the $HBrO_2$ concentration (x) is limited as noted above. However, this single difference is sufficient to change radically the flow topology of the system.

The Tyson model [29] has one ambiguous edge corresponding to a composite chemical system with 2 influence diagrams which are C_2+B_3 and B_2+C_3. If the turbulent vertex Y has logical structure, the flow topology of each of these two influence diagrams has a single attracting region. However, if the effect of the B_2 circuit in the B_2+C_3 influence diagram is suppressed by a low weight of the $x \rightarrow y$ directed edge through appropriate rate constant adjustment, the resulting C_3 system can have the flow topology appropriate for periodic oscillation. More significantly, however, appropriate interlocking cycle flow topology for a chaotic system *cannot* be generated from the Tyson model, which is based on the "Oregonator" suggested by Field and Noyes [32]. This may relate to the inability to find any range of chaotic behavior from simulation studies on related systems [33].

The Tomida and Tsuda model corresponds to a composite chemical system with 4 influence diagrams since it has two ambiguous edges. The flow topologies for these 4 influence diagrams cover all possibilities for the relevant family (Q in [23]) which, in particular, include the interlocking cycles required for chaos. In this connection Tomita and Tsuda [31] have found chaos in their model through computer simulation studies.

Experimental studies on the Belousov–Zhabotinskii reaction in a continuous-flow stirred reactor [6–8] suggest a well-defined flow rate range in which the oscilla-

tions are chaotic rather than periodic. The above analysis suggests that the second model in Table 4 (the model of Tomita and Tsuda [31]) more closely approximates such a chaotic system. A chemical implication of this observation is that reaction with the one-electron oxidant (Ce^{+4}) is significant in limiting the accumulation of autocatalytically generated $HBrO_2$. This is consistent with available information [30] on the potentials in oxybromine systems which suggest that the following reaction:

$$Ce^{+4} + BrO_2^- \rightleftharpoons Ce^{+3} + BrO_2\cdot \tag{3}$$

may proceed in either direction depending upon the conditions (e.g., acidity, ability of counterions to complex with cerium, etc.). Furthermore, these observations suggest a greater sensitivity of even the qualitative dynamics of the Belousov–Zhabotinskii reaction on the one-electron oxidant used (e.g., Ce^{+4} versus $(o\text{-phen})_3Fe^{3+}$) than is often assumed.

References

1. Nicolis, G., Portnow, J.: Chem. Revs. **73**, 365 (1973)
2. Noyes, R. M., Field, R. J.: Ann. Rev. Phys. Chem. **25**, 95 (1974)
3. Noyes, R. M.: Ber. Bunsenges. Phys. Chem. **84**, 295 (1980)
4. Schmitz, R. A., Graziani, K. R., Hudson, J. L.: J. Chem. Phys. **67**, 3040 (1977)
5. Hudson, J. L., Hart, M., Marinko, D.: J. Chem. Phys. **71**, 1601 (1979)
6. Hudson, J. L., Mankin, J. C.: J. Chem. Phys. **74**, 6171 (1981)
7. Lorenz, E. N.: J. Atmos. Sci. **20**, 130 (1963)
8. Rössler, O. E.: Z. Naturforsch. **31a**, 397 (1976)
9. Rössler, O. E.: Z. Naturforsch. **31a**, 1664 (1976)
10. Rössler, O. E.: Phys. Letters **57A**, 397 (1976)
11. Rössler, O. E.: Lect. Appl. Math. **17**, 141 (1979)
12. Rössler, O. E.: Ann. N. Y. Acad. Sci. **316**, 376 (1979)
13. Clarke, B. L.: J. Chem. Phys. **60**, 1481 (1974)
14. Clarke, B. L.: Advan. Chem. Phys. **43**, 1 (1980)
15. Caldwell, S. H.: Switching circuits and logical design. New York: Wiley 1958, 1967
16. Hu, S.-T.: Mathematical theory of switching circuits and automata. Berkeley and Los Angeles: California Press 1968
17. Glass, L., Kauffman, S. A.: J. Theor. Biol. **39**, 103 (1973)
18. Glass, L.: J. Theor. Biol. **54**, 85 (1975)
19. Glass, L.: J. Chem. Phys. **63**, 1325 (1975)
20. Glass, L.: in: Statistical mechanics, Pt. B. Berne, B. J. Ed. New York: Plenum Press 1977
21. Glass, L.: in: Statistical mechanics and statistical methods in theory and application, Landman, U. Ed. New York: Plenum Press 1977
22. Glass, L., Pasternack, J. S.: J. Math. Biol. **6**, 207 (1978)
23. King, R. B.: Theoret. Chim. Acta (Berl.) **56**, 269 (1980)
24. Thomas, R.: Kinetic logic. Berlin: Springer 1979
25. King, R. B.: J. Theor. Biol. **98**, 347 (1982)
26. Hirsch, M. W., Smale, S.: Differential equations, dynamical systems, and linear algebra. New York: Academic Press 1974
27. Robert, F. S.: Discrete mathematical models. Englewood Cliffs, New Jersey: Prentice-Hall 1973
28. Bornmann, L., Busse, H., Hess, B.: Z. Naturforsch. **28c**, 514 (1973)
29. Tyson, J. J.: Ann. N. Y. Acad. Sci. **316**, 279 (1979)

30. Field, R. J., Körös, E., Noyes, R. M.: J. Am. Chem. Soc. **94**, 8649 (1972)
31. Tomita, K., Tsuda, I.: Phys. Letters **71A**, 489 (1979)
32. Field, R. J., Noyes, R. M.: J. Chem. Phys. **60**, 1877 (1974)
33. Ganapathisubramanian, N., Noyes, R. M.: J. Chem. Phys. **76**, 1770 (1982)

Received January 19, 1983